Clays and Clay Minerals, Vol. 55, No. 1, 36–44, 2007.

PARTICLE PROPERTIES OF HYDROTHERMAL AMMONIUM-BEARING ILLITE-SMECTITE

VLADIMÍR ŠUCHA[1], PETER UHLÍK[1], JANA MADEJOVÁ[2], SABINE PETIT[3], IVAN KRAUS[1] AND L'UBICA PUŠKELOVÁ[4]

[1] Faculty of Natural Sciences, Comenius University, Mlynská dolina G, 842 15 Bratislava, Slovak Republic
[2] Institute of Inorganic Chemistry, Slovak Academy of Sciences, Dúbravská 9, Bratislava, Slovak Republic
[3] Université de Poitiers, CNRS UMR 6532, 40, av. du recteur Pineau, 86022 Poitiers, France
[4] Geological Institute, Slovak Academy of Sciences, Dúbravská 9, Bratislava, Slovak Republic

Abstract—Mixed-layer illite-smectite with high degree of ordering (rectorite-like clay) and with three types of interlayer cations – K^+, Na^+ and NH_4^+, was determined in the high-sulfide epithermal mineralization of the Western Carpathian Mountains. The tobelitic portion of the clay comprises 5–10%. Ammonium was detected both by chemical analysis and by Fourier transform infrared analysis. Some of the ammonium can be assigned to a poorly bound form, not fully fixed in the illitic interlayer. The finest size fraction separated from the samples behaves differently from the rest of the sample. It contains two layers of water molecules in the expandable interlayers as determined by X-ray diffraction, whereas coarser fractions have only one water layer in the interlayers.

Key Words—Ammonium Illite-smectite, Carpathian Mountains, Hydrothermal Activity, Particle Properties, Rectorite-like Mineral.

INTRODUCTION

The NH_4^+ cation has similar properties to K^+, and therefore can often be found in the mica interlayers as a cation compensating permanent mica layer charge. Trace concentrations of NH_4^+ can always be detected in mica structures (Jia and Kerrich, 2000; Papineau *et al.*, 2005), but our interest is focused on clay minerals where the tobelitic fraction represents at least a few percent.

The clear relationship between ammonium and organic matter explains the abundant occurrence of NH_4 in the structure of sedimentary micas connected with organic matter at all stages of maturation, either as a major element or as a trace cation (Juster *et al.*, 1987; Daniels and Altaner, 1990; Cooper and Abedin, 1991; Williams and Ferrell, 1991; Compton *et al.*, 1992; Šucha *et al.*, 1994; Drits *et al.*, 1997; Nieto, 2002; Papineau *et al.*, 2005, *etc.*). Much less frequently, the presence of ammonium is reported from hydrothermal environments. The first complete description of ammonium mica where >90% of mica interlayers are occupied by ammonium (clear tobelite) was reported by Kozáč *et al.* (1977) from Vihorlat Mts in the Western Carpathians. Later, Higashi (1978, 1982) described ammonium mica from Japan. Tobelite from hydrothermally altered black shales in Utah was described by Wilson *et al.* (1992). The most complete set of hydrothermal tobelites and mixed-layer tobelite-smectite minerals was described from Hargita Mts (Romania) by Bobos *et al.* (1995) and Bobos and Gerghari (1999).

* E-mail address of corresponding author:
sucha@fns.uniba.sk
DOI: 10.1346/CCMN.2007.0550103

In this paper we present new data on ammonium-bearing rectorite-like minerals found in a hydrothermal field in Slovakia. The main goal of the paper is to describe this special clay and the interesting properties of its finest size fractions.

MATERIALS

Ammonium-bearing illite-smectites were collected from a hydrothermal field in the Western Carpathians, situated in the Miocene volcanic region of Banská Štiavnica (Central Slovakia, Figure 1). The Banská Štiavnica hydrothermal region is a large hydrothermal field created by two epithermal systems that produced disseminated base-metal and vein mineralization (see review by Štohl *et al.*, 1994).

Part of the hydrothermal region where ammonium-bearing clay was found is of high-sulfidation origin (according to Hedenquist *et al*., 1996) and belongs to the caldera filling which belongs to the second volcanic phase (Konečný *et al.*, 1983; Konečný and Lexa, 1998). It is composed of large, hydrothermally silicified bodies associated with advanced argillic zones dominated by pyrophyllite, kaolinite and $2M_1$ illite. Large pyrite contents were determined in both silicified bodies and clays (Uhlík and Šucha, 1997). Ammonium-bearing clay was identified at three localities in the filling of the Banská Štiavnica stratovolcano (Figure 1). Localities 1 and 2 are outcrops where samples were collected from shallow drill-holes (up to 5 m deep). Material from both localities is macroscopically identical. The rock is friable and fine grained with larger (mm–cm) sized pieces of quartzite and disintegrated andesite. The color is gray or reddish-brown depending on the degree of

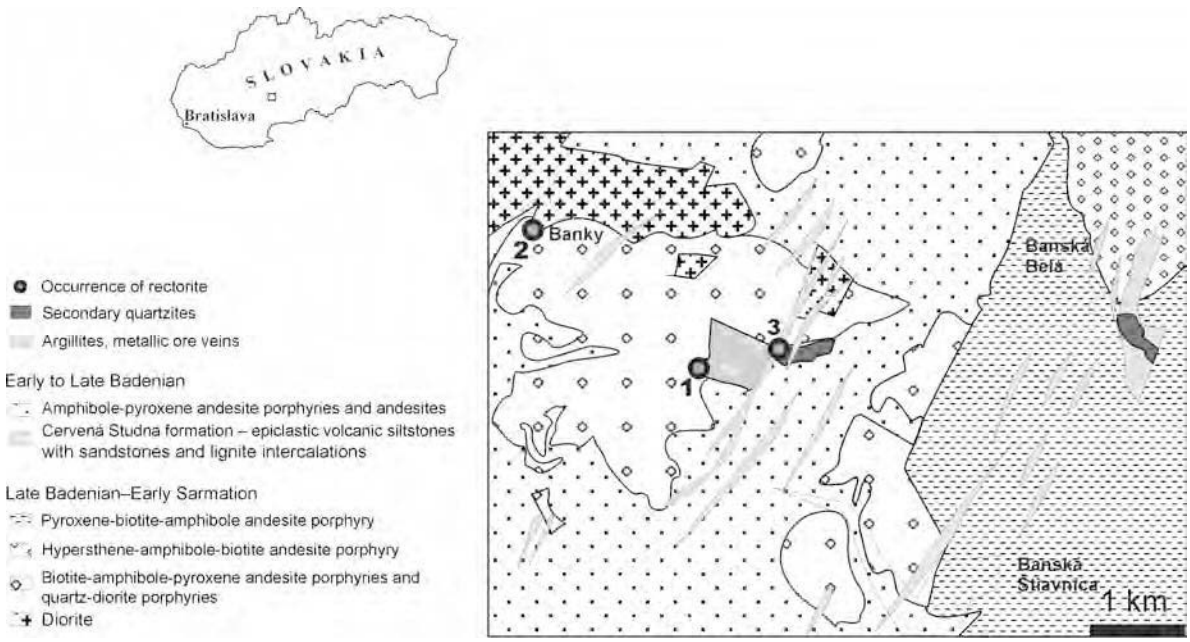

Figure 1. Simplified geological position of the ammonium-bearing I-S occurrences situated NE of Banská Štiavnica (according Konečný and Lexa, 1998). 1 – Červená Studňa, 2 – Banky, 3 – Šobov.

weathering of pyrite. Locality 3 is an open quartzite mine situated in the largest quartzite body of the formation (Uhlik and Šucha, 1997). The rock is relatively hard, and white to light gray in color.

METHODS

Clay samples were dried at room temperature, gently disintegrated to pass a 0.16 mm sieve and used for chemical and mineralogical determinations.

The clay size fractions (<0.2, 0.2–1.0, 1.0–2.0, <2.0, 2.0–5.0 μm) were separated from bulk samples by centrifugation in distilled water. Prior to fractionation, the samples were dispersed in an ultrasonic bath for 5 min and subsequently treated with Na acetate buffer, H_2O_2 and Na dithionite (Jackson, 1975) to remove organic matter and Fe, Mn oxides. Excess soluble salts were removed by centrifugation followed by dialysis.

X-ray diffraction (XRD) analyses of oriented and random specimens were carried out using a Philips PW 1710 diffractometer with CuKα radiation and a graphite monochromator. Traces were recorded from specimens in an air-dried state and saturated with ethylene glycol overnight at 70ºC. The scan-step for all the analyses was 0.02º2θ and count time varied between 1 and 5 s per step.

Both the <0.2 and 0.2–2 μm fractions of the bulk samples were Sr saturated (4 × 1 N $SrCl_2$ followed by washing in distilled water and dialysis) and analyzed chemically. Si was determined gravimetrically, whereas Al, Mg, Fe, Ca, K, Na and Sr were analyzed by atomic absorption spectrometry and atomic emission spectrometry. NH_4 was determined by means of steam distillation, according to Bremner (1965). Cation exchange capacity (CEC) was calculated from the Sr content assuming that all Sr is exchangeable.

A small portion of the samples was saturated with NH_4Cl before and after Li treatment including Li saturation and overnight heating in a Pt crucible at 300ºC. Clay samples saturated with LiCl and NH_4Cl were washed until no excess salts were detected. NH_4Cl-saturated samples were used for estimation of the octahedral and tetrahedral charge distribution according to the technique by Petit *et al.* (1998).

The Fourier transform infrared (FTIR) spectra were obtained using a Nicolet Magna 750 spectrometer. The KBr pressed-disc technique (1 mg of sample and 200 mg of KBr) was used for the transmission measurements. Diffuse reflectance infrared Fourier transform (DRIFT) spectra were obtained from powders using a diffuse reflectance accessory 'Collector' from Spectra-Tech. Spectra were acquired either on the pure sample or following dilution with KBr (sample/KBr ratio 1:1)

Electron microscope images were taken from ultra-thin sections of samples embedded in Spurr resin using a JEOL JEM-2000 FX microscope operated at 160 kV. Prior to embedding, small pieces of clay were coated with agar and saturated with water for 3 days. Water was replaced by methanol, methanol by propylene oxide and finally Spurr resin was applied (Tessier, 1984). Sections 60–70 nm thick were cut using a diamond knife and a Reichert Ultracut microtome. Images were taken at 60,000 × magnifications. The chemical compositions of individual particles were determined using a Link AN

https://doi.org/10.1346/CCMN.2007.0550103 Published online by Cambridge University Press

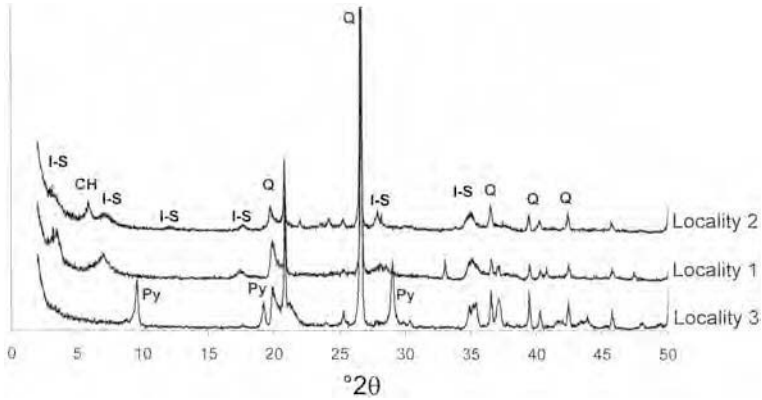

Figure 2. Bulk-rock XRD patterns of samples containing ammonium-bearing illite-smectite from three studied localities. I-S – mixed-layer illite-smectite, Py – pyrophyllite, CH – chlorite, Q – quartz.

10000 energy-dispersive analyzer with a windowless Si-Li detector connected to a Philips 420 STEM microscope operated at 120 kV (for more details see Romero *et al.*, 1992). Specimens were prepared by the sedimentation of the suspension onto copper grids already covered by collodium and carbon films to support clay particles.

RESULTS AND INTERPRETATIONS

Mineral composition determined by XRD

The bulk-rock mineral composition of localities 1 and 2, determined by XRD, is dominated by quartz, feldspars and clays with significant pyrite content which is often weathered in reddish rocks to Fe oxyhydroxides. The bulk-rock composition of locality 3 is dominated by quartz and pyrophyllite (Figure 2).

The clay fraction of all samples from localities 1 and 2 is dominated by a regularly interstratified illite-smectite mineral with ~50% expandable layers. Mixed-layer I-S is also present at locality 3, but pyrophyllite is the most abundant mineral phase there (Figure 3). The expandability of I-S in all samples was determined using the peak-position method (Środoń, 1980) of EG-saturated XRD patterns and compared with Newmod©-calculated (Reynolds, 1985) patterns. The I-S is a regularly interstratified clay very similar to rectorite in structure but it is not ideal rectorite because there is a variation in expandability (of ~50%) and peak positions are slightly different from those calculated by Newmod© for a true rectorite.

Some samples contain small amounts of Al-rich chlorite (estimated from the distribution of the intensities of 00l reflections) in the clay fraction. Chlorite is slightly more abundant in samples from locality 2, but no other significant differences were found between samples from these two localities when air dried and EG saturated.

Differences were determined when various size fractions of the same sample were compared. In all studied samples from localities 1 and 2, XRD patterns of air-dried specimens of small size fractions (<0.2 μm) were significantly different from those for larger size fractions (>0.2 μm). The first two peaks for the smaller fraction were shifted towards two larger values and an additional peak appeared between 17 and 18°2θ (Figure 4a). All differences between size fractions disappeared when the sample was saturated by EG (Figure 4b), indicating the difference in water content in

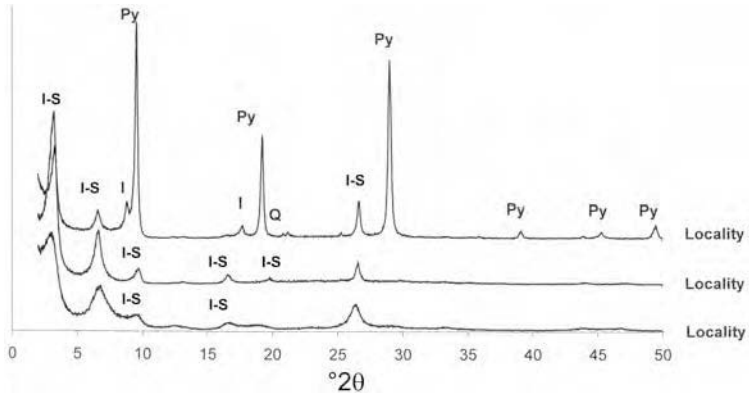

Figure 3. XRD patterns of the <2 μm clay fraction from oriented specimens saturated by EG from the studied localities. I-S – mixed-layer illite-smectite, Py – pyrophyllite, I – illite, Q – quartz.

https://doi.org/10.1346/CCMN.2007.0550103 Published online by Cambridge University Press

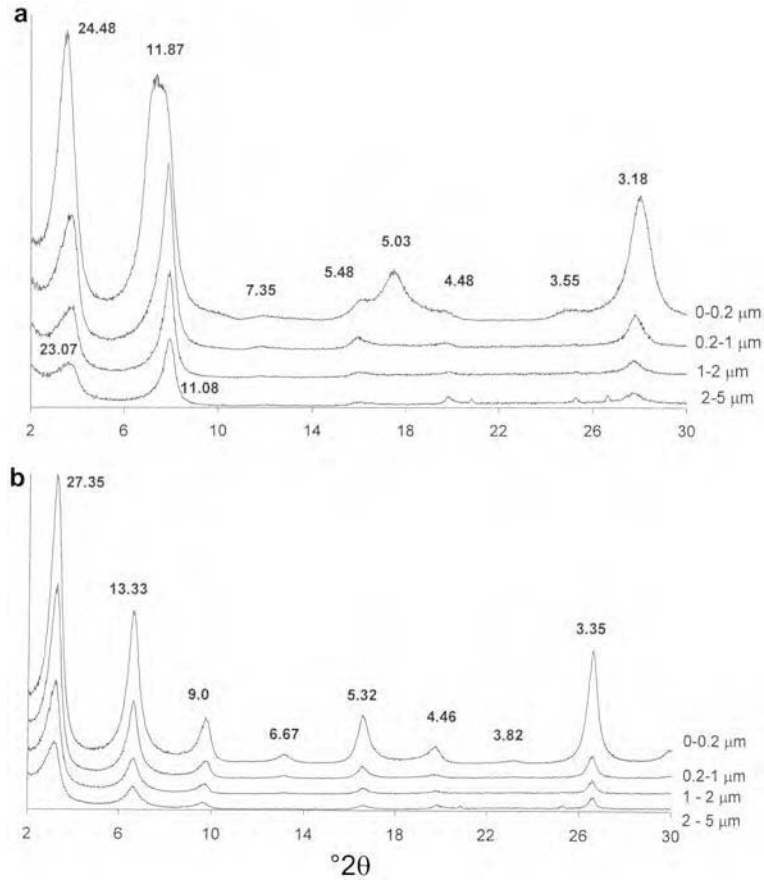

Figure 4. (a) XRD patterns of air-dried oriented specimens of sample 4487 from locality 1 separated into four different size fractions. (b) Same specimens X-rayed after EG saturation. Spacings in Å.

the interlayer space of expandable interlayers. Newmod©-calculated patterns of air-dried R1 interstratified I-S minerals with one or two layers of water molecules in the interlayer suggest that the difference is mainly due to this fact (Figure 5). To find out more precisely if the effect appears in other fractions as well, four different size fractions (0–0.2, 0.2–1, 1–2, 2–5 μm) of the same sample (monomineral sample from locality 1) were separated and X-rayed (Figure 4a,b). The special characteristics observed in

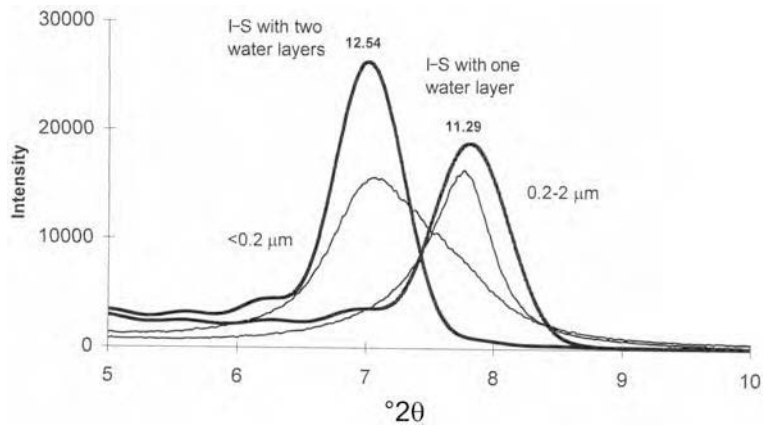

Figure 5. Comparison of XRD patterns of two different size fractions (0–0.2 and 0.2–2 μm) recorded in an air-dried state with the Newmod© computer model (bold lines) of mixed-layer I-S clay with one and two layers of water molecules in the expandable interlayers, respectively

https://doi.org/10.1346/CCMN.2007.0550103 Published online by Cambridge University Press

the <0.2 μm fraction were not detected in other size fractions. The only difference is the intensity of the peaks, which decreases with the increase in the size fraction of the sample. Peak intensity is a function of the number of clay crystals present in the size fraction.

Infrared spectroscopy

All samples show FTIR spectra of mixed-layer illite-smectite with characteristic stretching (ν) and bending (δ) vibrations of OH and Si-O groups (Figure 6). Moreover, a weak but clearly resolved band near 1400 cm^{-1} with a shoulder near 1430 cm^{-1} appeared in spectra of the samples obtained by the KBr pressed-disc technique. The absorptions in this region are attributed to the bending vibrations of the NH_4^+ cation and confirm the presence of NH_4^+ in the structure of the samples (Chourabi and Fripiat, 1981). The shoulder near 1430 cm^{-1} corresponds to NH_4^+ ions hydrogen bonded to the clay structure (Chourabi and Fripiat, 1981; Petit *et al.*, 1999; Pironon *et al.*, 2003). The absorption band near 1400 cm^{-1} indicates that during pellet preparation, the NH_4^+ ions from the clay mineral are exchanged with K^+ from KBr. Similar spectral features were reported for NH_4^+-saturated smectites, *i.e.* minerals containing exchangeable NH_4^+ ions (Petit *et al.*, 1999). However, all exchangeable cations in the mixed-layer illite-smectite were replaced by Sr^{2+}, thus the NH_4^+ ions were supposed to occur in illite layers as non-exchangeable cations.

To determine whether KBr causes replacement of NH_4^+ by K^+ in mixed-layer illite-smectite, DRIFT measurements were performed and compared to KBr pellets. These measurements allow sample analysis with or without dilution with KBr. The spectrum of the undiluted sample shows a broad band near 1435 cm^{-1} (Figure 7a). After dispersion of the sample in KBr, the shape of the NH_4^+ bending band remained almost the same (Figure 7b). However, the DRIFT spectrum of the sample mixed with KBr (ratio 1:1) and ground intensively in an agate mortar shows a component near 1400 cm^{-1} (Figure 7c). These changes confirm that grinding of the mixed-layer illite-smectite with KBr, either in the course of the pellet preparation or DRIFT experiments, is responsible for the replacement of NH_4^+ by K^+. Ammonium release indicates that the ammonium in the illite structure was not very strongly bonded, although it was not in an exchangeable position (samples were treated as described in the methods and recorded both in Na^+- and Sr^{2+}-forms).

Ammonium sorption combined with Li sorption, according to the technique described by Petit *et al.* (1998), was used to determine possible differences in the layer-charge distribution in the samples. The integral intensity of the ammonium band of NH_4-exchanged clays was measured before and after Li fixation. Li fixed either in octahedral sites or in pseudo-hexagonal sites reduces the layer charge (Bujdak *et al.*, 2002; Czimerova *et al.*, 2004) so this was applied to identify the possible differences between two size fractions. The intensity measurement before Li treatment represents the total CEC of the sample, whereas measurement after the treatment is assigned to tetrahedral charge, and octahedral charge-related sorption is obtained as a difference between total and tetrahedrally related CEC (Petit *et al.*, 1998). Figure 8 shows the result of the measurement of two size fractions of three samples. The total CEC of the finer fraction is larger, related to greater expandability. The data show that more of the sorbed ammonium of both size fractions is related to tetrahedral charge rather than to octahedral charge.

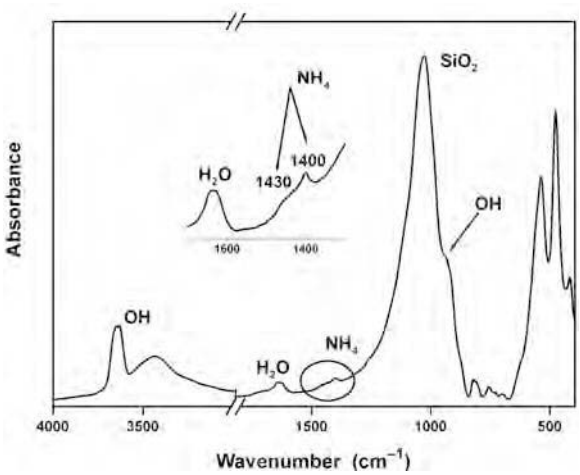

Figure 6. FTIR spectrum of the ammonium-bearing I-S, obtained using the KBr pellet technique.

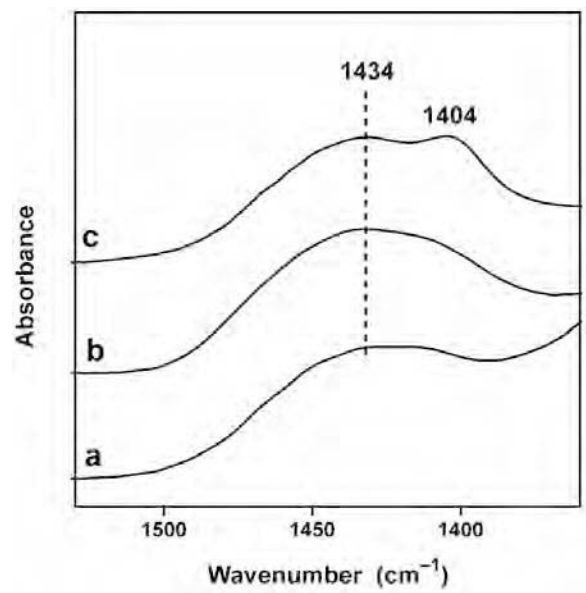

Figure 7. DRIFT spectrum of the undiluted sample (a); of the sample diluted with KBr and ground slightly (b); and of the sample heated at 300ºC overnight, diluted with KBr and ground (c).

https://doi.org/10.1346/CCMN.2007.0550103 Published online by Cambridge University Press

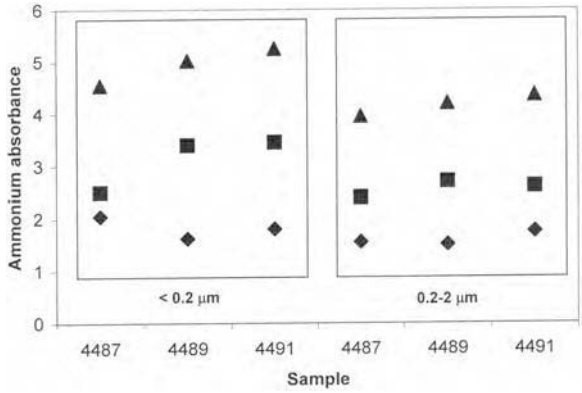

Figure 8. Distribution of layer charge as determined by the ammonium sorption technique of Petit *et al.* (1999). Triangles – total charge, equivalent to the total CEC; squares – CEC related to the tetrahedral charge; diamonds – CEC related to the octahedral charge.

Chemical composition

Three monomineral samples from locality 1 were used to determine the chemical composition of the clay fraction. Both size fractions (0–0.2 and 0.2–2 μm) were analyzed to reveal the chemical composition of the mixed-layer I-S and to detect possible differences between them. Compositions and structural formulae are listed in Table 1. All analyzed samples have very similar chemical compositions with large Al content and very small Fe content.

The presence of K, Na and NH_4 was attributed to fixed cations of the illite interlayer. We are not able to distinguish whether fixed cations are equally distributed in all interlayers or they form separate homoionic interlayers. However, for the sake of simplicity we assigned the fixed K, Na and NH_4 contents to theoretical homoionic interlayers, which we refer to as illitic, paragonitic and tobelitic phases. Theoretical illitic and paragonitic components are dominant and the tobelitic portion only reaches ~5–10%.

When comparing two size fractions, almost no difference can be found in the chemical composition of the clay tetrahedral and octahedral structures. Small differences are detected in the sum of the fixed interlayer cations, and in the exchangeable Sr and water contents

Table 1. Chemical composition of three monomineral ammonium-bearing illite-smectites from locality 1.

Sample	4487 (0.2–2 μm)	4487 (<0.2 μm)	4489 (0.2–2 μm)	4489 (<0.2 μm)	4491 (0.2–2 μm)	4491 (<0.2 μm)
SiO_2	54.45	55.45	55.77	56.46	55.40	55.58
Al_2O_3	37.11	36.26	35.96	35.09	35.79	36.14
Fe_2O_3	0.13	0.25	0.37	0.40	0.35	0.35
MgO	0.94	0.95	1.38	1.57	1.60	1.66
CaO	0.03	0.04	0.05	0.05	0.05	0.05
Na_2O	1.37	1.33	1.44	1.35	1.56	1.24
K_2O	3.49	2.97	2.45	2.05	2.60	1.76
SrO	2.38	2.62	2.44	2.88	2.46	3.04
NH_4	0.10	0.13	0.14	0.16	0.18	0.18
Sum	100	100	100	100	100	100
CEC	46	51	47	56	47	59
Crystallochemical formulae						
Si	6.75	6.79	6.93	6.91	6.89	6.91
Al	1.25	1.21	1.07	1.09	1.11	1.09
Al	3.86	3.84	3.76	3.75	3.72	3.74
Fe	0.01	0.02	0.03	0.03	0.03	0.03
Mg	0.17	0.17	0.25	0.28	0.29	0.3
Na	0.33	0.32	0.35	0.32	0.37	0.3
K	0.55	0.47	0.38	0.32	0.41	0.29
NH_4	0.04	0.05	0.06	0.06	0.07	0.07
Sr	0.17	0.18	0.18	0.2	0.18	0.22
Percentage of interlayer occupancy						
Na	36	38	44	46	44	45
K	60	56	48	46	48	44
NH_4	4	6	8	8	8	11
Fix	0.92	0.84	0.79	0.7	0.85	0.66
%Sfix	46	50	53	58	50	60

Both size fractions were analyzed for each sample. The CEC was calculated from the Sr content. Fix = the sum of the fixed cations in the illite interlayer; %Sfix = the expandability calculated from the fixed cations content (according to Środoń *et al.*, 1992).

https://doi.org/10.1346/CCMN.2007.0550103 Published online by Cambridge University Press

measured as the weight loss after drying at 105ºC. These differences are interrelated and connected to the slightly greater expandability of the smaller size fraction. Expandability (maximum expandability) was calculated from the total sum of the cations fixed in the interlayer (Środoń *et al*., 1992) and it ranges between 46 and 60% (Table 1). The maximum difference in expandability between the size fractions is 10%. Consequently, greater expandability leads to greater water content in the sample and to a larger amount of exchangeable Sr. The CECs of all analyzed samples were calculated from the Sr content because samples were analyzed in Sr-saturated form (Table 1).

The chemical compositions of the individual particles of the two size fractions were determined by analytical electron microscopy (AEM). Figure 9 shows that the data are consistent with the chemical composition presented in Table 1. The AEM revealed no differences between the two size fractions.

Particle-thickness distribution

The particle thickness of one illite-smectite sample was measured using high-resolution transmission electron microscopy (HRTEM) images. The distribution calculated from measurements (Figure 10) shows that 2 nm-thick bilayers (two 2:1 layers with fixed interlayer cations) are dominant, but a significant number of monolayers (one 2:1 layer) and thicker particles are also present. It confirms the XRD expandability measurements which indicate that the clay is not ideal rectorite.

DISCUSSION

Ammonium-bearing clay was detected in three localities. Two localities (1, 2) have the same mineral composition, and the third, situated in a quartzite deposit, has a different mineral composition with quartz and pyrophyllite as the dominant phases, which could indicate a different origin. The presence of pyrophyllite could indicate significantly greater temperatures (Hamley *et al.* 1980; Eberl 1979a, 1979b) than those expected for the origin of illite-smectite having an expandability of ~50% (Šucha *et al.*, 1992, 1993; Uhlík and Majzlan, 2004). We suggest that the formation of the ammonium-bearing clay represents a separate phase of argillic hydrothermal alteration of the particular region related to fluids with greater ammonium content. We could consider the formation of ammonium-bearing clay as being younger than the formation of pyrophyllite.

The presence of slightly different properties in the clay's finest size fraction, represented by a larger number of water layers in the expandable interlayers, can be interpreted as the effect of particle surfaces. Different water contents in the interlayers are documented by XRD but it is difficult to speculate about its origin. The outcomes of all techniques described earlier did not confirm any significant difference between relevant size fractions except a small CEC difference which is clearly related to a number of expandable interlayers – greater in the smaller fraction.

The FTIR bands at 1400 and 1430 cm^{-1} recorded after grinding clay with KBr show the effect of KBr on ammonium binding to the clay structure. The band at 1400 cm^{-1} has been reported several times in the literature (Chourabi and Fripiat, 1981; Petit *et al.*, 1999; Pironon *et al.*, 2003) as a band related to the exchangeable ammonium. We did not observe this band previously when we studied other ammonium-bearing illites mixed with KBr (anchimetamorphic and synthetic ammonium illites, published by Šucha *et al.,* 1994, 1998). Previously published spectra were recorded on illites in the same way as those presented here. The main difference is in mean crystal thickness. The previous NH_4-bearing illites were of much larger mean crystal thickness than those described here (2 nm thick illite crystals were dominant in the previous work). Thus we think that smaller mean crystal thickness may cause a release of the ammonium not exchangeable by standard treatment with 1 N Na or Sr chloride during sample preparation.

CONCLUSIONS

Based on XRD, FTIR and chemical analyses, the presence of ammonium-bearing illite-smectite with R1 ordering and composition close to rectorite (both Na and K are fixed in the illite interlayers) was determined in

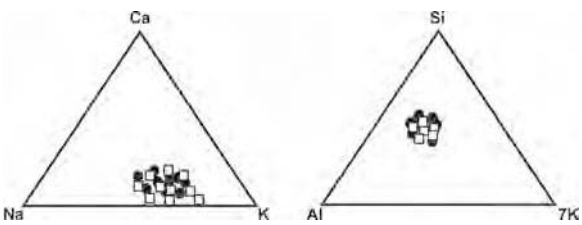

Figure 9. Chemistry of individual clay particles as analyzed by AEM: circles – 0–0.2 μm fraction; squares –0.2–2 μm fraction.

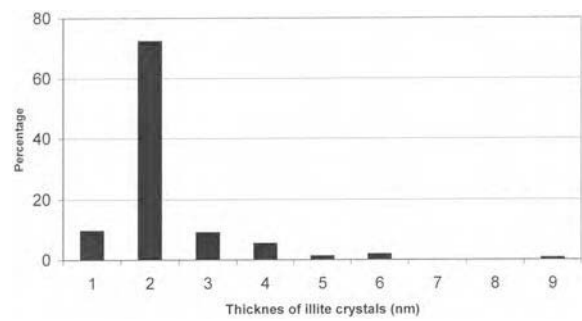

Figure 10. Distribution of the particle-size thickness as measured by HRTEM.

https://doi.org/10.1346/CCMN.2007.0550103 Published online by Cambridge University Press

hydrothermally altered rocks of the Červená Studňa formation from the Banská Štiavnica Mts. (Slovakia).

The FTIR data show that not all ammonium is fixed in the illite but that a significant portion could be released when mixed with KBr. This ammonium could be located at the edges of illite crystals and thus readily exposed to the reaction with KBr.

The finest size fraction (<0.2 μm) of the illite-smectite samples probably has different surface properties, leading to the presence of two layers of water molecules in the smectite interlayer determined by the XRD, whereas the coarser fractions have only one layer of water molecules. No other technique was able to detect differences between size fractions.

ACKNOWLEDGMENTS

This study was supported by the Slovak Grant Agency VEGA (project N. 1/0009/03). Many thanks to Maria Čaplovičová and Francoise Elsass for the assistance with HRTEM analyses and to D.D. Eberl for reading the manuscript. The authors appreciate very much the constructive remarks by reviewers Lynda B. Williams and Boris Sakharov.

REFERENCES

Bobos, I. and Ghergari, L. (1999) Conversion of smectite to ammonium illite in the hydrothermal system of Harghita Bai, Romania: SEM and TEM investigations. *Geologica Carpathica*, **50**, 379–387

Bobos, I., Šucha, V. and Soboleva, S. (1995) Mixed-layer ammonium illite-smectite and ammonium illite from hydrothermal system Hargita Bai, The East Carpathians (Romania). *Euroclay 95 Abstracts volume*, Leuven, p. 384.

Bremner, J.M. (1965) Inorganic forms of nitrogen. Pp. 1179–1237 in: *Methods of Soil Analysis* (C.A. Black, editor). American Society of Agronomy, Madison, Wisconsin.

Bujdak, J., Iyi, N. and Fujita, T. (2002) Aggregation and stability of 1,1‘-diethyl-4,4‘-cyanine dye on the surface of layered silicates wit different charge densities. *Colloids and Surfaces A*, **207**, 207–214.

Chourabi, B. and Fripiat, J.J. (1981) Determination of tetrahedral substitutions and interlayer surface heterogeneity from vibrational spectra of ammonium in smectites. *Clays and Clay Minerals*, **29**, 260–268.

Compton, J.S., Williams, L.B. and Ferrell, R.E., Jr (1992) Mineralization of organogenic ammonium in the Monterey Formation, Santa Maria and San Joaquin basins, California, USA. *Geochimica et Cosmochimica Acta*, **56**, 1979–1991.

Cooper, J.E. and Abedin, K.Z. (1981) The relationship between fixed ammonium-nitrogen and potassium in clays from a deep well on the Texas Gulf Coast. *Texas Journal of Science*, **33**, 103–111.

Czimerova, A., Jankovic, L. and Bujdak, J. (2004) Effect of the exchangeable cations on the spectral properties of methylene blue in clay dispersion. *Journal of Colloid and Interface Science*, **274**, 126–132.

Daniels, E.J. and Altaner, S.P. (1990) Clay mineral authigenesis in coal and shale from the Anthracite region, Pennsylvania. *American Mineralogist*, **75**, 103–111.

Drits, V.A., Lindgreen, H. and Salyn, A.L. (1997) Determination of the content and distribution of fixed ammonium in illite-smectite by X-ray diffraction: Application to North Sea illite-smectite. *American Mineralogist*, **82**, 79–87.

Eberl, D.D. (1979a) Reaction series for dioctahedral smectite: the synthesis of mixed-layer pyrophyllite/smectite. *Proceedings of International Clay Conference*, Oxford, 1978, pp. 375–383.

Eberl, D.D. (1979b) Synthesis of pyrophyllite polytypes and mixed layers. *American Mineralogist*, **64**, 1091–1096.

Hamley, J.J., Montoya, J.W., Marinenko, J.W. and Luce, R.W. (1980) Equilibria in the system Al_2O_3-SiO_2-H_2O and some general implications for alteration/mineralization processes. *Economic Geology*, **75**, 210–228.

Hedenquist, J.W., Izawa, E., Arribas, A., Jr. and White, N.C. (1996) Epithermal gold deposits: Styles, characteristics, and exploration. *Resource Geology Special Publication* **1**.

Higashi, S. (1978) Dioctahedral mica minerals with ammonium ions. *Mineralogical Journal*, **9**, 16–27.

Higashi, S. (1982) Tobelite, a new ammonium dioctahedral mica. *Mineralogical Journal*, **11**, 138–146.

Jackson, M.L. (1975) *Soil Chemical Analysis – Advanced Course*, 2nd edition. Published by the author, Madison, Wisconsin, 895 pp.

Jia, Y. and Kerrich, R. (2000) Giant quartz vein systems in accretionary orogenic belts: the evidence for a metamorphic fluid origin from delta ^{15}N and delta ^{13}C studies. *Earth and Planetary Science Letters*, **184**, 211–224.

Juster, T.C., Brown, P.E. and Bailey, S.W. (1987) NH_4-bearing illite in very low-grade metamorphic rocks associated with coal, Northeastern Pensylvania. *American Mineralogist*, **72**, 555–565.

Konečný, V. and Lexa, J. (1998) *Geological map of the region Štiavnické vrchy Mts. and Pohronsk Inovec Mts. 1:50 000.* GSSR, Bratislava.

Konečný, V., Lexa, J. and Planderová, E. (1983) Stratigraphy of the neovulcanites from the Central Slovakia. *Zapadne Karpaty, series. Geology*, **9**, GÚDŠ, Bratislava, 1–203.

Kozáč, J., Očenáš, D. and Derco, J. (1977) Ammonium hydromica from Vihorlat Mts. *Mineralia Slovaca*, **9**, 479–494 (in Slovak).

Nieto, F. (2002) Characterization of coexisting NH_4- and K-micas in very low-grade metapelites. *American Mineralogist*, **87**, 205–216.

Papineau, D., Mojzsis, S.J., Karhu, J.A. and Marty, B. (2005) Nitrogen istopic composition of ammoniated phyllosilicates: case studies from Precambrian metamorphosed sedimentary rocks. *Chemical Geology*, **216**, 37–58.

Petit, S., Righi, D., Madejová, J. and Decarreau, A. (1998) Layer charge estimation of smectites using infrared spectroscopy. *Clay Minerals*, **33**, 579–591.

Petit, S., Righi, D., Madejová, J. and Decarreau, A. (1999) Interpretation of the infrared NH_4^+ spectrum of the NH_4^+-clays: application to the evaluation of the layer charge. C*lay Minerals*, **34**, 543–549.

Pironon, J., Pelletier, M., De Donato, P. and Mosser-Ruck, R. (2003) Characterization of smectite and illite by FTIR spectroscopy of NH_4^+ interlayer cations. *Clay Minerals*, **38**, 201–211.

Reynolds, R.C. (1985) *NEWMOD, a computer program for the calculation of basal X-ray diffraction intensities and mixed-layered clays*. R.C. Reynolds, Hanover, New Hampshire, USA.

Romero, R., Robert, M., Elsass, F. and Garcia, C. (1992) Evidence by electron microscopy of weathering microsystems in soil formations developed from crystalline rocks. *Clay Minerals*, **27**, 21–33.

Środoń, J. (1980) Precise identification of illite/smectite interstratifications by X-ray powder diffraction. *Clays and Clay Minerals*, **28**, 401–411.

Środoń, J., Elsass, F., McHardy, W.J. and Morgan, D.J. (1992) Chemistry of illite-smectite inferred from TEM measure-

ments of fundamental particles. *Clay Minerals*, **27**, 137–158.

Štohl, J., Lexa, J., Kaličiak, M. and Bacsó, Z. (1994) Origin of polymetallic mineralization in neogene volcanoclastics of the Western Carpathians. *Mineralia Slovaca*, **26**, 75–117 (in Slovak).

Šucha, V., Kraus, I., Mosser, Ch., Hroncová, Z., Soboleva, K.A. and Širáňová, V. (1992) Mixed-layer illite/smectite from Dolná Ves hydrothermal deposit, Kremnica Mountains, The West Carpathians. *Geologica Carpathica Clays*, **43,** 13–19.

Šucha, V., Kraus, I., Gerthofferová, H., Peteš, J. and Sereková, M. (1993) Smectite to illite conversion in bentonites and shales of the East Slovak Basin. *Clay Minerals*, **28**, 243–253.

Šucha, V., Kraus, I. and Madejová, J. (1994) Ammonium illite from anchimetamorphic shales associated with anthracite in the Zemplinicum of the Western Carpathians. *Clay Minerals*, **29**, 369–377.

Šucha, V., Elsass, F., Eberl, D.D., Madejová, J., Kuchta, L., Gates, W.P. and Komadel, P. (1998) Hydrothermal synthesis of ammonium illite. *American Mineralogist*, **83**, 58–67.

Tessier, D. (1984) Étude experimental de l'organisation des materiaux argileux. Dr. Science thesis, Universite Paris VII, INRA publication, 361 pp.

Uhlík, P. and Majzlan, J. (2004) Conditions of mixed-layer illite-smectite formation at the deposit Dolná Ves on the southwest margin of Kremnica stratovolcano. *Mineralia Slovaca*, **36**, 331–338.

Uhlík, P. and Šucha, V. (1997) Distribution of pyrophyllite in the Sobov deposit and comparison of its properties with the pyrophyllite from Viglasska Huta. *Mineralia Slovaca*, **29**, 73–79.

Williams, L.B. and Ferrell, R.E., Jr. (1991) Ammonium substitution in illite during maturation of organic matter. *Clays and Clay Minerals*, **39**, 400–408.

Wilson, P.A., Parry, W.T. and Nash, W.P. (1992) Characterization of hydrothermal tobelitic veins from black shale, Oquirrh Mountains, Utah. *Clays and Clay Minerals*, **40**, 405–420.

(*Received 2 August 2005; revised 3 September 2006; Ms. 1086; A.E. Douglas K. McCarty*)